

GENERAL-PURPOSE SLIDING-MODE CONTROLLER FOR DC/DC CONVERTER APPLICATIONS

P.Mattavelli L.Rossetto G.Spiazzi

Department of Electrical Engineering, University of Padova
Via Gradenigo 6/a - 35131 Padova - ITALY
Tel:(+39)49-828.7500 Fax:828.7599

P.Tenti

Department of Electronics and Informatics, University of Padova
Via Gradenigo 6/a - 35131 Padova - ITALY
Tel:(+39)49-828.7600 Fax:828.7699

Abstract. A general-purpose sliding-mode controller is described, which can be applied to most dc/dc converter topologies. It has same circuit complexity as standard current-mode controllers, but provides extreme robustness and speed of response against supply, load and parameter variations. Moreover, contrary to other sliding-mode techniques, the proposed solution features constant switching frequency in the steady-state, synchronization to external triggers, and absence of steady-state errors in the output voltage.

I. INTRODUCTION

The control of dc/dc converters has been widely investigated in the past. Many control techniques have been proposed and analyzed. Among them, the most popular are *Voltage Control* and *Current Injected Control* (and its derivations like *Standard Control Module* and *Average Current Control*) [1]. Controllers based on these techniques are simple to implement and easy to design, but their parameters generally depend on the working point. Achieving large-signal stability often calls for a reduction of the useful bandwidth, affecting converter performances. Moreover, application of these techniques to high-order dc/dc converters, e.g. Cuk and Sepic topologies, may result in very critical design of control parameters and difficult stabilization.

Another approach, which complies with the non-linear nature of these converters, is based on control techniques derived from the variable structure systems (VSS) theory, like sliding-mode (SM) control [2-4].

As known, SM control offers several advantages: stability even for large supply and load variations, robustness, good dynamic response, simple implementation. Conversely, SM control has some drawbacks: first, due to its hysteretic nature, the switching frequency varies depending on the working point; second, steady-state errors can affect the controlled variables; third, selection of control parameters may be difficult due to the complexity of the sliding-mode control theory.

This paper describes a general-purpose SM controller, useful for any basic dc/dc converter structure, which overcomes the above drawbacks. In fact:

- switching frequency is kept constant in the steady state, making possible synchronization to external triggers; instead,

frequency may vary during transients, so as to ensure stability and speed of response;

- steady-state errors are eliminated;
- control tuning is easy;
- circuitry is simple;
- in addition, switch current limitation can easily be implemented.

The proposed controller was tested with several dc/dc converter topologies, i.e. Buck, Boost, Buck-boost, Cuk and Sepic. Excellent converter performances were found, showing considerable improvements over Current-Mode control techniques.

II. PRINCIPLES OF SLIDING-MODE CONTROL

The general SM control scheme of dc/dc converters is shown in Fig.1. U_i and u_{CN} are input and output voltages, respectively, while i_{Li} and u_{Cj} ($i=1+r$, $j=r+1+N-1$) are the internal state variables of the converter (inductor currents and capacitor voltages). Switch S accounts for the system non-linearity and indicates that the converter may assume only two linear sub-topologies, each associated to one switch status. All dc/dc converters having this property (including all single-switch topologies, plus push-pull, half and two-level full-bridge converters) are represented by the equivalent scheme of Fig.1. The above condition also implies that the mathematical approach presented here is valid only for *continuous conduction mode* (CCM) operation.

In the scheme of Fig.1, according to the general SM control theory, all state variables are sensed, and the corresponding errors (defined by difference to the steady-state values) are multiplied by proper gains K_i and added together to form the sliding function ψ . Then, hysteretic block HC maintains this function near to zero, so that we can write:

$$\psi = \sum_{i=1}^N K_i \cdot \epsilon_i = 0 \quad (A)$$

where N is the system order (number of state variables).

Observe that (1) represents a hyperplane in the state error space, passing through the origin. Each of the two regions separated by this plane is associated, by block HC, to one

converter substructure. If we assume (*existence condition* of the SM) that the state trajectories near the surface, in both regions, are directed toward the sliding plane, we can enforce the system state to remain near (lie on) the sliding plane by proper operation of the converter switch(es).

Control design. In practice, SM controller design only requires a proper selection of the sliding surface (1), i.e. of coefficients K_i , so as to ensure:

- the *existence condition* mentioned above;
- the *hitting condition*, which requires that the system trajectories encounter the sliding plane irrespective of their starting point in the state space;
- *stability* of the system trajectories on the sliding plane.

Other constraints derive from the specified dynamic behavior.

From a practical point of view, selection of the sliding surface is not difficult if second-order converters are considered. In this case, in fact, the above conditions can be verified by simple graphical techniques [4]. For higher order converters, like Cuk and Sepic, a more general approach must be used [5,6].

Advantages. Due to its property of acting on all system state variables simultaneously, sliding-mode control offers several benefits:

- First, let N be the system order, system response has order $N-1$. In fact, under sliding mode only $N-1$ state variables are independent, the N -th being constrained by (1).
- Second, system dynamic is very fast, since all control loops act concurrently.
- Third, stability (even for large input and output variations) and robustness (against load, supply and parameter variations) are excellent, as for any other hysteretic control.
- Fourth, system response depends only slightly on actual converter parameters.

Disadvantages. Conventional SM control techniques have the following drawbacks:

- First, switching frequency varies depending on the working point.
- Second, output voltage may be affected by steady-state errors.
- Third, all state variables must be sensed.

The first problem arises from the fact that the switching frequency depends on the rate of change of function ψ and on the amplitude of the hysteresis band. Since ψ is a linear combination of state-variable errors, it depends on actual converter currents and voltages, and its behavior is difficult to predict. Thus, stabilization of the switching frequency can only be obtained by modulating the hysteresis band amplitude (e.g. by means of a Phase Locked Loop), but this solution increases the circuit complexity, and does not maintain constant frequency during transients.

The second problem derives from the fact that inductor current references and capacitor voltage references are difficult to evaluate, since they generally depend on load power demand, supply voltage and load voltage. To overcome this problem, in practical implementations all state variable errors, except for the output voltage, are computed using high-pass filters. This implies that, in the steady state, all error variables ϵ_i , except ϵ_N ,

have zero average value; thus, if sliding function ψ , due to the hysteretic control, has non-zero average value, a steady-state output voltage error necessarily appears.

The third problem would make unpractical this control technique with high-order converters. However, it has already been proved that excellent performances can be obtained even with reduced-order controllers [5,6].

III. GENERAL-PURPOSE SLIDING-MODE CONTROL SCHEME

The proposed general-purpose SM controller scheme is shown in Fig.2. As we can see, only two state variables are sensed: the output voltage and one inductor current. This latter is the inductor current for 2nd order schemes, i.e. Buck, Boost, Buck-Boost, and the input inductor current for 4th order schemes, i.e. Cuk and Sepic.

This scheme eliminates the above drawbacks, according to the following provisions.

A. Elimination of steady-state errors.

As already mentioned, current error ϵ_i is computed by means of a high-pass filter, while output voltage error ϵ_u is obtained by comparison with reference signal u_0^* . A PI action is introduced on sliding function ψ in order to eliminate its dc value, thus reducing the dc value of the output voltage error to zero. In practice, the integral part of this regulator is enabled only when the system is on the sliding surface; in this way, the system behavior during transients, when ψ can reach values far from zero, is not affected, thus maintaining the fast response of SM control.

B. Switching frequency stabilization.

In order to provide stabilization of the switching frequency, a proper ramp signal w at the desired frequency f_w is added to function ψ . If, in the steady-state, the amplitude of w is predominant in ψ , a commutation occurs at any cycle of w , thus making the switching frequency equal to f_w . This also allows converter synchronization to external triggers. Instead, under dynamic conditions, error terms ϵ_i and ϵ_u increase, w is overridden, and the system retains the excellent dynamic response of the sliding mode.

C. Current limitation.

Additional functions can be implemented to provide switch or inductor current limitation. For instance, the current limiter shown in Fig.2 overrides sliding-mode control when the switch current exceeds threshold I_{lim} . If this happens, the control maintains the switch current at the value I_{lim} .

Note lastly that the scheme of Fig.2 has the same complexity of a standard Current-Mode control.

IV. CONTROLLER DESIGN

In this section, guidelines for the choice of all controller parameters are given.

As regards the power stage components, they can be selected on the basis of power/ripple requirements only.

A. Selection of coefficients K_i , K_u .

The detailed procedure for selecting coefficients K_i and K_u is given in [5] for Cuk converters, and [6] for Sepic converters. Here only a brief review is reported with reference to these fourth-order structures. Similar considerations apply also to any other converter topologies.

The basic schemes of Cuk and Sepic converters are shown in Fig.3. According to the variable structure systems theory, the converter equations must be written in the following form:

$$\dot{\underline{x}} = \underline{A}\underline{x} + \underline{B}\sigma + \underline{G}B \quad (2)$$

where σ is the switch status, and \underline{x} represents the vector of state variable errors, given by:

$$\underline{x} = \underline{v} - \underline{V}^*C \quad (3)$$

Here $\underline{v}=[i_1, i_2, u_1, u_2]^T$ is the state variable vector, and $\underline{V}^*=[I_1^*, I_2^*, U_1^*, U_2^*]^T$ is the vector of their dc references (index T means transposition).

Matrices \underline{A} , \underline{B} , \underline{G} are given in Appendix I for Sepic and Cuk converters.

Existence condition. We assume that the sliding function ψ is a linear combination of state variables i_1 and u_2 , given by:

$$\psi = \underline{K}^T \bullet \underline{x} D \quad (4)$$

where $\underline{K}^T=[K_i, 0, 0, K_u]$ is the vector of the sliding coefficients. The purpose of the hysteretic control is to maintain $\psi \approx 0$, which means that the state trajectories evolve on the sliding plane $\psi=0$.

Assuming that the switch is kept on ($\sigma=1$) when ψ is negative and off ($\sigma=0$) when ψ is positive, we may express the existence condition in the form [2]:

$$\frac{\partial \psi}{\partial t} = \underline{K}^T \underline{A}\underline{x} + \underline{K}^T \underline{G} < 0 \quad 0 < \psi < \xi \quad (5.a)$$

$$\frac{\partial \psi}{\partial t} = \underline{K}^T \underline{A}\underline{x} + \underline{K}^T \underline{B} + \underline{K}^T \underline{G} > 0 \quad -\xi < \psi < 0 \quad (5.b)$$

where ξ is an arbitrary small positive quantity.

Note that equations (5) simply tell us that when the switch is *off* function ψ must increase, while when it is *on* ψ must decrease.

Hitting condition. If the sliding mode exists, a sufficient condition is [2]:

$$\underline{K}^T \underline{A}_4 \leq 0 E \quad (6)$$

where \underline{A}_4 is the 4-th column of matrix \underline{A} .

Stability condition. Using the equivalent input approach [2], and taking into account constrain (1), the system behavior in sliding mode can be expressed by:

$$\dot{\underline{x}} = \underline{A}'\underline{x} + \underline{G}'F \quad (7)$$

As mentioned before, the system order is N-1 (N-1=3 for Sepic and Cuk converters), where matrix \underline{A}' is non linear. After linearization around the working point \underline{X} , we obtain:

$$\dot{\underline{x}} = \underline{A}''(\underline{X})\underline{x} + \underline{G}''(\underline{X})G \quad (8)$$

From (8), the system eigenvalues are recursively calculated as a function of coefficients K_i and K_u in order to find the solutions having eigenvalues with negative real part and suitable

damping factor. It is important to note that, due to the condition $\psi = 0$, only the ratio between K_i and K_u is important.

In practice, several solutions are generally found. Those ensuring stability and good dynamic response, and satisfying (5) and (6), are then selected.

B. Selection of other control parameters.

High-pass filter time constant τ_{HPF} .

The choice of τ_{HPF} can heavily affect the system behavior, in terms of both speed and damping of the response. τ_{HPF} must be suitably higher than the switching period, to pass the ripple at the switching frequency, but small enough to allow a fast converter response.

In practice, values close to the natural time constants of the system give the best results.

PI regulator time constant τ_{PI} .

Selection of this parameter is not critical, because the PI regulator is enabled only when the system status lies on the sliding surface; accordingly, it does not affect the system dynamic during transients.

In practice τ_{PI} can be set equal to τ_{HPF} .

Ramp signal w .

This signal enforces a constant switching frequency when the system status lies on the sliding plane, irrespective of input voltage and load variations. For this purpose, the ramp amplitude is selected taking into account the slope of function ψ during the off period and the hysteresis band amplitude, so that function ψ_f hits the lower part of the hysteresis band at the end of the ramp, causing the commutation. For example, Fig.4 shows simulated waveforms of w , ψ_{PI} , and ψ_f signals in the case in which the ramp slope is greater than the slope of ψ .

V. EXPERIMENTAL RESULTS

Two prototypes were built, a Cuk converter and a Sepic converter. The basic schemes are shown in Fig.3a and Fig.3b, respectively, their parameters being listed in table I.

TABLE I
CONVERTER PARAMETERS
CUK

$U_g = 24V$	$I_{lim} = 1.5A$
$U_2 = 15V$	$f_s = 50KHz$
$L_1 = 3.3mH$	$L_2 = 2.2mH$
$R_1 = 1\Omega$	$R_2 = 0.5\Omega$
$C_1 = 100\mu F$	$C_2 = 47\mu F$
$R_L = 15 \div 150\Omega$	$\tau_{HPF} = 0.15mS$
$K_i = 1.2$	$\tau_{PI} = 0.15mS$
$K_u = 1$	

SEPIC

$U_g = 15V$	$I_{lim} = 3.5A$
$U_2 = 20V$	$f_s = 50KHz$
$L_1 = 700\mu H$	$L_2 = 380\mu H$
$R_1 = 1\Omega$	$C_2 = 100\mu F$
$C_1 = 6.8\mu F$	$R_L = 20 \div 200\Omega$
$K_i = 1.1$	$\tau_{HPF} = 0.5mS$
$K_u = 1$	$\tau_{PI} = 0.5mS$
$n = 1.5$	

A. Cuk converter.

Since a complete analysis and experimental verification has already been reported in [5] (for the case of a second-order sliding-mode control without frequency stabilization), here only the step-load variation response is considered. The corresponding output voltage waveforms are shown in Fig.5 together with the switch gate signal. This latter shows clearly how the SM control works: after the load is disconnected, the switch S remains open, so that the overshoot in u_2 is due only to the energy stored in L_2 ; when the load is reapplied, the switch is kept closed for a while in order to transfer the maximum energy to the output stage.

B. Sepic converter.

A more extensive analysis is reported with reference to the Sepic. Fig.6 shows output voltage and input current during start-up under no-load condition. The overshoot on the output voltage is about 10% of the nominal value; decreasing the current limit I_{lim} , it is possible to lower it to as low as 5%.

The converter behavior in the case of a step load change, is reported in Fig.7. Besides u_2 and i_1 waveforms, also variable ψ_f is shown. We can observe that, when the load is disconnected, ψ_f goes out of the hysteresis band; consequently, the switch S remains open and the converter operates in DCM (*Discontinuous Conduction Mode*). In this way, no energy goes to the output, because the diode D is off. Then, when the load is connected again, the system remains on the sliding surface, continuously switching to cope with the load request.

A significant reduction of the voltage overshoot can be obtained by clipping signal ϵ_i to a suitable value, which forces the converter to work in the Discontinuous Conduction Mode almost immediately after the load disconnection.

C. Comparison between SM control and Current-Mode control in the case of Sepic converters.

Current-Mode control design for Sepic topology is not easy. Differently from simpler converter topologies, the transfer function between duty-cycle and switch current has a bad phase behavior. Consequently, a damping network (R_d - C_d) in parallel to capacitor C_1 may become necessary.

In our case, no ramp compensation was used, so as to maximize the current loop gain.

Fig.8 shows behavior under SM control (Fig.8a) and Current-Mode control (Fig.8b), in the case of a step-load variation from full-load to no-load and vice-versa. SM control shows better performances, both in terms of overshoot and response speed. For the sake of comparison, the damping network R_d - C_d has been maintained also for the SM control, although it is not needed. Still, it is important to observe that this behavior is only slightly better than that obtained without the damping network (as shown by Fig.7), while Current-Mode control, in the same situation, becomes unstable. This fact reveals the robustness of SM control, confirmed also by the good behavior shown for input voltage variations of as much as $\pm 30\%$. On the contrary, decreasing the input voltage with Current-Mode control makes the system unstable, without ramp compensation.

As a measure of the converter audiosusceptibility, the output voltage ripple due to 100Hz input voltage variations was

measured for both controller types: an improvement of 7dB (from -20dB to -27dB) was obtained with SM control.

VI. CONCLUSIONS

A general-purpose sliding-mode controller for dc/dc converters is presented. This controller, which has the same complexity of standard current-mode controllers, can be applied to almost all dc/dc converter topologies.

This approach has several advantages: stability even for large supply and load variations, robustness and good dynamic behavior. Moreover, it provides constant switching frequency in the steady state, allowing synchronization to external triggers, and no steady-state errors in the output voltage.

Although experimental results have been presented for Cuk and Sepic converters only, the approach demonstrated to be effective also for more simple Buck, Boost, and Buck-Boost topologies.

A comparison with Current-Mode control shows the superiority of the proposed solution.

APPENDIX I

With reference to (2), matrices \underline{A} , \underline{B} , \underline{G} , for Sepic and Cuk converters, are given as follows:

Sepic converter.

$$\underline{A} = \begin{bmatrix} -\frac{R_1}{L_1} & 0 & -\frac{1}{L_1} & -\frac{1}{nL_1} \\ 0 & 0 & 0 & -\frac{1}{nL_2} \\ \frac{1}{C_1} & 0 & 0 & 0 \\ \frac{1}{nC_2} & \frac{1}{nC_2} & 0 & -\frac{1}{R_L C_2} \end{bmatrix} \quad (\text{A.1a})$$

$$\underline{B} = \begin{bmatrix} \frac{u_1 + u_2/n}{L_1} \\ \frac{L_2}{i_1 + i_2} \\ \frac{C_1}{i_1 + i_2} \\ \frac{1}{nC_2} \end{bmatrix} \quad (\text{A.1b})$$

$$\underline{G} = \begin{bmatrix} \frac{-R_1 I_1^* + U_i - (U_1^* + U_2^*/n)}{L_1} \\ \frac{U_2^*}{nL_2} \\ \frac{I_1^*}{C_1} \\ \frac{(I_1^* + I_2^*)/n - U_2^*/R_L}{C_2} \end{bmatrix} \quad (\text{A.1c})$$

Cuk converter.

$$\underline{A} = \begin{bmatrix} -\frac{R_1}{L_1} & 0 & -\frac{1}{L_1} & 0 \\ 0 & -\frac{R_2}{L_2} & 0 & -\frac{1}{L_2} \\ \frac{1}{C_1} & 0 & 0 & 0 \\ 0 & \frac{1}{C_2} & 0 & -\frac{1}{R_L C_2} \end{bmatrix} \quad (\text{A.2a})$$

$$\underline{B} = \begin{bmatrix} \frac{u_1}{L_1} \\ \frac{u_1}{L_2} \\ \frac{-i_1 - i_2}{C_1} \\ 0 \end{bmatrix} \quad (\text{A.2b})$$

$$\underline{G} = \begin{bmatrix} \frac{U_i - R_1 I_1^* - U_1^*}{L_1} \\ \frac{-R_2 I_2^* - U_2^*}{L_2} \\ \frac{I_1^*}{C_1} \\ \frac{I_2^* - (U_2^*/R_L)}{C_2} \end{bmatrix} \quad (\text{A.2c})$$

ACKNOWLEDGMENT

The authors would like to thank Dr.M.Magrin and Dr.L.Bianchin, whose dedicated work made possible experimental tests.

Thanks are also due to Mr.R.Sartorello, who supervised experimental activities.

REFERENCES

- [1] - R.Redl, N.Sokal, "Current-Mode control, five different types, used with the three basic classes of power converters: small-signal AC and large-signal DC characterization, stability requirements, and implementation of practical circuits", IEEE-PESC, 1985, pp. 771-785.
- [2] - V.I.Utkin, *Sliding modes and their application in variable structure systems*, MIR Publishers, Moscow, 1974.
- [3] - U.Itkis, *Control systems of variable structure*, J.Wiley and Sons, New York, 1976.
- [4] - R.Venkataramanan, A.Sabanovic, S.Cuk: "Sliding-mode control of DC-to-DC converters". Publ. of Power Electronic Group, CalTech, 1986.
- [5] - L.Malesani, L.Rossetto, G.Spiazzi, P.Tenti, "Performance optimization of Cuk converters by sliding-mode control," IEEE APEC, 1992, pp.395-402.
- [6] - P.Mattavelli, L.Rossetto, G.Spiazzi, P.Tenti, "Sliding-mode control of SEPIC converters", ESPC'93, in press.

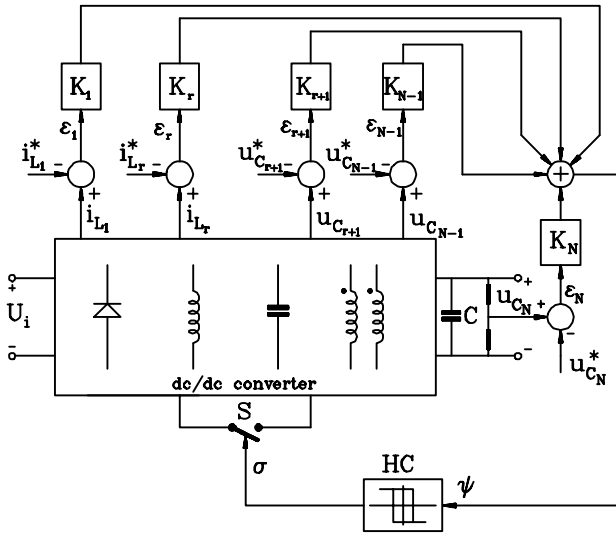


Fig.1 Principle scheme of a SM controller applied to a generic dc/dc converter.

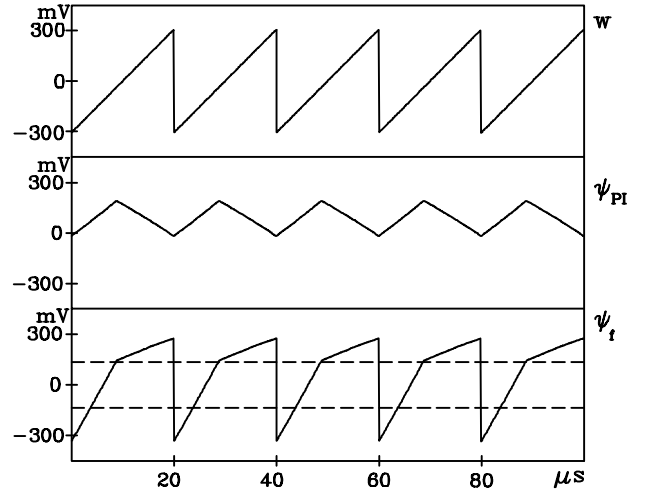


Fig.4 Simulated waveforms of ramp w , ψ_{PI} and ψ_f signals.

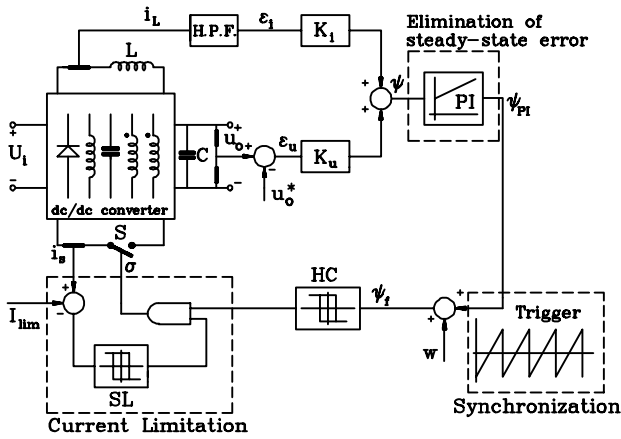


Fig.2 General-purpose SM controller scheme.

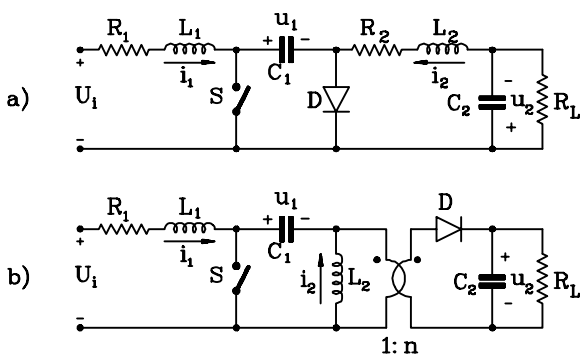


Fig.3 a) Cuk converter; b) Sepic converter.

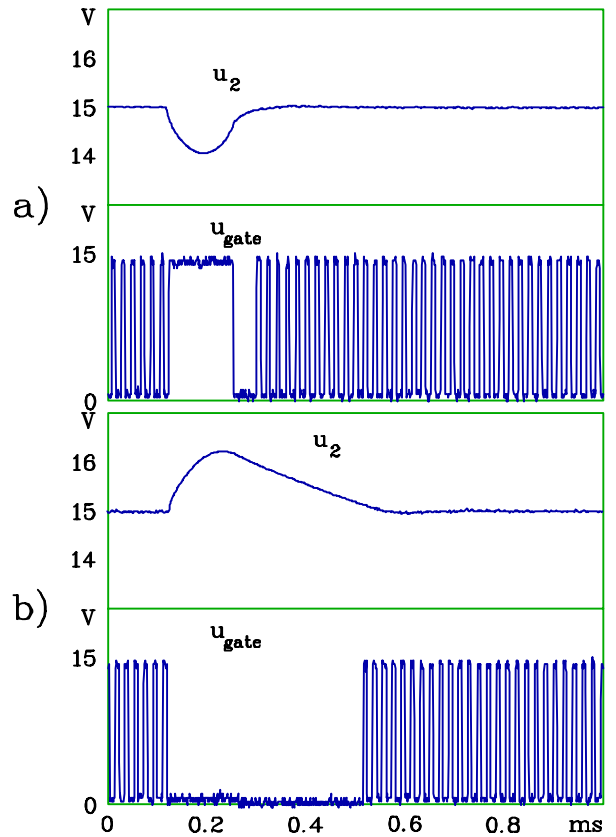


Fig.5 Output voltage u_2 and switch gate waveforms for step load variation a) from no-load to full-load; b) from full-load to no-load.

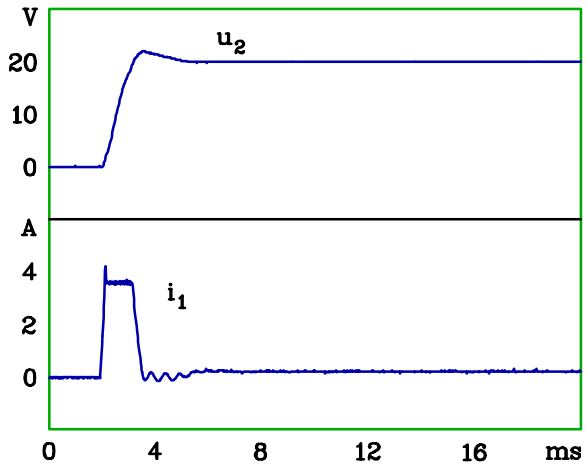


Fig.6 Output voltage and input current during start-up, at no-load.

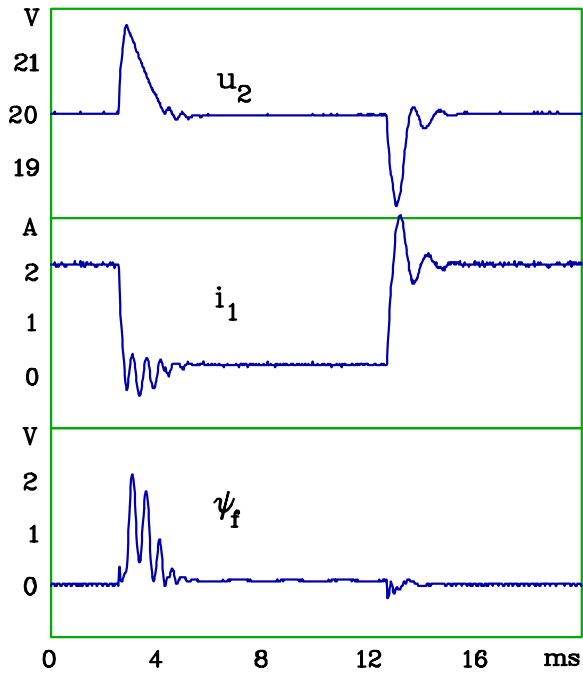


Fig.7 Waveforms for step load variation.

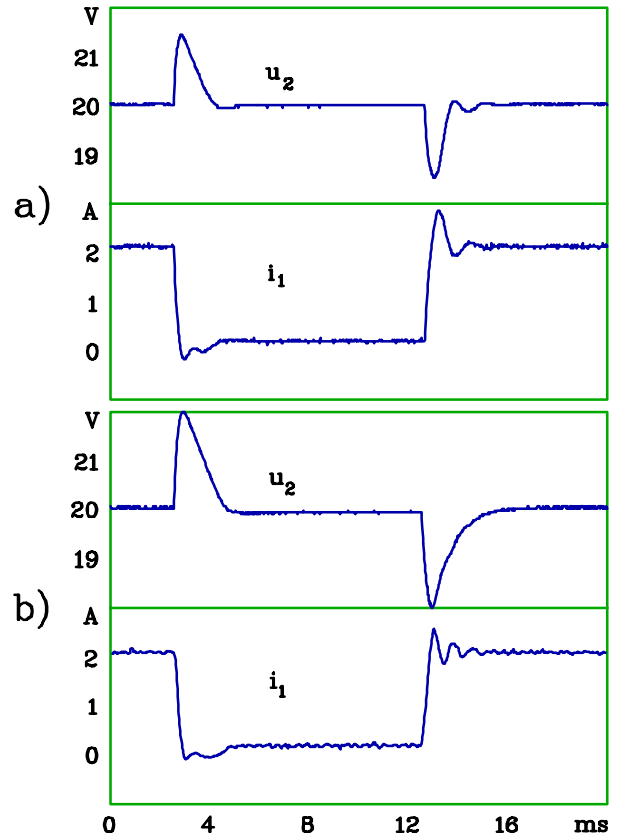


Fig.8 Output voltage and input current waveforms for step load variation:
a) SM control; b) Current-Mode control.